

pre-print, then published in *Macromolecules* 2017, 50, 6586–6594 - DOI: 10.1021/acs.macromol.7b01214

This document is confidential and is proprietary to the American Chemical Society and its authors. Do not copy or disclose without written permission. If you have received this item in error, notify the sender and delete all copies.

Efficient modulation of polyethylene microstructure by proper activation of (α -diimine)Ni(II) catalysts: synthesis of well performing polyethylene elastomers.

Journal:	<i>Macromolecules</i>
Manuscript ID	Draft
Manuscript Type:	Article
Date Submitted by the Author:	n/a
Complete List of Authors:	D'Auria, Iliaria; Università degli Studi di Salerno , Dipartimento di Chimica e Biologia "A. Zambelli" Maggio, Mario; Università degli Studi di Salerno, Chemistry and Biology Guerra, Gaetano; University of Salerno, Chemistry and Biology Pellecchia, Claudio; Università di Salerno, Chemistry & Biology

SCHOLARONE™
Manuscripts

1
2
3
4
5
6
7 Efficient modulation of polyethylene microstructure
8
9
10
11 by proper activation of (α -diimine)Ni(II) catalysts:
12
13
14
15
16 synthesis of well performing polyethylene
17
18
19
20 elastomers.
21
22
23
24
25

26 *Ilaria D'Auria, Mario Maggio, Gaetano Guerra,* and Claudio Pellecchia**
27

28
29
30 Dipartimento di Chimica e Biologia "A. Zambelli", Università di Salerno,
31

32
33 via Giovanni Paolo II, 132 - 84084 Fisciano (SA) Italy
34
35
36
37
38
39

40 ABSTRACT.
41

42
43 The activation of a prototypical nickel(II) Brookhart catalyst by either methylalumoxane
44 (MAO) or diethylaluminumchloride (AlEt_2Cl) under a variety of conditions showed that a
45
46 proper choice of the mode of activation is a powerful tool to modulate the polymer
47
48 microstructure. In particular, use of AlEt_2Cl instead of MAO resulted in the production of
49
50 more branched polyethylenes with a higher content of long chain branches and even some
51
52 "branches on branches". Characterization of these materials by NMR, thermal, X-ray
53
54
55
56
57
58
59
60

1
2
3 diffraction and mechanical analyses provided insight in the relationships between the
4
5 microstructure and the crystallization behavior and the elasticity of the polymers. For
6
7 these branched polyethylenes, a transition from plastomeric toward elastomeric behaviour
8
9 occurs for branch concentrations much lower than for ethylene-propylene copolymers and
10
11 like those observed for ethylene copolymers with bulkier comonomers. For elastomeric
12
13 materials, reduction of branch concentration implies two relevant advantages: i) reduction
14
15 of glass transition temperature becoming closer to that of polyethylene; ii) more efficient
16
17 radical crosslinking with reduction of degradation reactions. An additional advantage is, of
18
19 course, a polymer production process involving only ethylene.
20
21
22
23
24
25
26
27
28
29
30
31
32
33
34
35
36
37
38
39
40
41
42
43
44
45
46
47
48
49
50
51
52
53
54
55
56
57
58
59
60

INTRODUCTION

The discovery of a novel class of catalysts based on Ni(II) or Pd(II) α -diimine compounds by Brookhart *et al.* in 1995¹ was a main breakthrough for the development of late transition metal and "post-metallocene" olefin polymerization catalysts.²⁻¹¹ The unique feature of these catalysts resides in their ability to promote a "chain-walking" mechanism of polymerization, a process involving a number of β -hydride eliminations and reinsertions with opposite regiochemistry.^{1,12-15} In the case of ethylene polymerization, this mechanism results in the production of macromolecules with a variable content of branches of different lengths, methyl branches being the most abundant, affording polymers ranging from semicrystalline plastics to thermoplastic elastomers to hyperbranched amorphous waxes and oils. For Ni catalysts, as shown already in the first Brookhart's reports,^{1,12-15} the degree of branching is a function of temperature, monomer pressure and catalyst structure: an increase of polymerization temperature results in higher branching, while an increase of monomer pressure produces the opposite effect; finally, an increase of the steric bulk in the axial positions of the square-planar coordination sphere produces higher branching and plays a decisive role for the achievement of high molecular weight polymers. These findings were thoroughly explained by a mechanism involving a cationic 16-electron β -agostic Ni(II) complex as the resting catalyst state (in equilibrium with the alkyl ethylene complex) for which the relative rates of chain-walking and monomer coordination are affected by temperature, pressure and the steric hindrance of the ligand (note that for Pd catalysts the degree of branching is always higher and independent on monomer pressure since the catalyst resting state is the alkyl ethylene complex).¹²⁻¹⁵

1
2
3 In the following 20 years, hundreds of studies by researchers from both academia and industry
4 have flourished building upon these concepts, introducing a large number of variants in the
5
6
7
8 ligand design and substantially confirming and extending Brookhart's initial findings.¹⁶⁻²¹
9

10
11 Some 20 years ago, we reported that the degree of branching is also significantly influenced by
12
13 co-catalyst effects,²² but this finding was apparently overlooked, although some subsequent
14
15
16 studies discussed this issue, with contrasting conclusions.²³⁻²⁷ Here we report the results
17
18 concerning the performance of a prototypical bis(arylimino)acenaphthene dibromo nickel(II)
19
20 Brookhart catalyst (**1**, chart 1) activated by either methylalumoxane (MAO) or
21
22 diethylaluminumchloride (AlEt₂Cl) under variable conditions, confirming that the polymer
23
24 microstructure is substantially affected by the mode of activation. More interestingly, we found
25
26 that high molecular weight amorphous polyethylenes displaying excellent elastomeric properties
27
28 can be produced under suitable conditions.²⁸⁻³⁰ Full characterization of these materials by
29
30 structural, thermal, mechanical analyses provides insight in relationships between microstructure,
31
32
33
34
35 crystallization behavior and elasticity of these branched polymers.
36
37
38

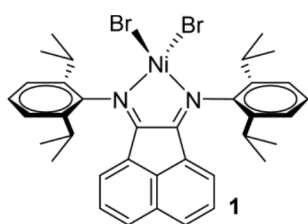


Chart 1.

EXPERIMENTAL SECTION

General procedures

1
2
3 All manipulation involving air and/or moisture-sensitive compounds were performed under an
4 atmosphere of nitrogen in a Braun Labmaster glovebox or using Schlenk techniques. Glassware
5 used were dried in an oven at 120 °C overnight and exposed three times to vacuum–nitrogen
6 cycles. Toluene and *o*-dichlorobenzene were refluxed over metallic sodium, dichloromethane
7 was refluxed over CaH₂ and hexane was refluxed over sodium-benzophenone. They were
8 distilled under nitrogen before use. Deuterated solvents were purchased from Aldrich and stored
9 in the glovebox over 3 Å molecular sieves before use. All other reagents were purchased from
10 Aldrich and used as received. Ethylene was purchased from SON and used without further
11 purification. Complex 1, bis(arylimino)acenaphthene dibromo nickel(II) was synthesized
12 according to the literature.^{1,31,32}

27 28 Characterization Techniques

29
30
31 The NMR spectra were recorded at 373K on a Bruker 600 MHz Ascend 3 HD spectrometers.
32
33 Chemical shifts (δ) were expressed as parts per million. ¹H NMR spectra were referenced using
34 the residual solvent peak at δ 6.85 for C₂Cl₄D₂ (TCDE) and δ 7.91 for C₆D₄Cl₂ (*o*-DCB).
35
36

37
38
39 ¹³C NMR spectra were obtained on a Bruker 600 MHz Ascend 3 HD spectrometer in a 5 mm
40 probe on *o*-dichlorobenzene-d₄ solutions of polymers locked at 100°C using a 90° pulse of 12 μ s,
41 a spectral width of 12 kHz (80 ppm), a relaxation delay of 4 s, an acquisition time of 5 s. ¹³C
42 NMR spectra were referenced internally to the major backbone methylene carbon resonance,
43 which was taken as 30.00 ppm from Me₄Si.
44
45
46
47
48
49
50

51
52 SEC measurements for some representative samples were carried out by using an integrated
53 GPCV2000 SEC system from Waters equipped with two on-line detectors: 1) a differential
54 viscometer (DV); 2) a differential refractometer (DRI) as concentration detector. The
55
56
57
58
59
60

1
2
3 measurements were made at 145 °C using 1,2-dichlorobenzene as a solvent. Every value was the
4
5 average of two independent measurements, using an universal calibration (SEC-CU) constructed
6
7 from 18 narrow MMD polystyrene standards, with the molar mass ranging from 162 to $5.48 \times$
8
9 10^6 g/mol. For sample 5, $M_w = 215000$, $M_w / M_n = 3.9$; for sample 6, $M_w = 87000$, $M_w / M_n =$
10
11 2.2.
12
13

14
15
16 DSC measurements were carried out under nitrogen in the temperature range $-120^{\circ}\text{C} + 170^{\circ}\text{C}$, at
17
18 heating or cooling rates of $10^{\circ}\text{C}/\text{min}$, on a TA instruments (DSC 2920).
19
20

21
22 Wide-angle X-ray diffraction (WAXD) patterns of unstretched samples were obtained by an
23
24 automatic Bruker D8 Advance diffractometer, operating in the $\theta/2\theta$ Bragg–Brentano geometry,
25
26 at 35 kV and 40 mA, using the nickel filtered $\text{Cu-K}\alpha$ radiation (1.5418°A). A degree of
27
28 crystallinity (X_c) has been determined by resolving the diffraction patterns, in a selected 2θ range
29
30 (7° – 32°), into two areas A_c and A_a that are taken as proportional to the crystalline and amorphous
31
32 fractions of br-PE. The degree of crystallinity is then calculated as $X_c = 100 A_c / (A_c + A_a)$. As a
33
34 reference fully amorphous X-ray diffraction pattern, the pattern of the sample with 68% of
35
36 branches, was used.
37
38
39

40
41
42 Wide-angle X-ray diffraction patterns of the stretched films were obtained by a D8 QUEST
43
44 Bruker diffractometer ($\text{CuK}\alpha$ radiation) sending the X-ray beam perpendicular to the film
45
46 surface. For stretched films, the *degree of axial orientation* (χ), that is of the orientation of the
47
48 chain axes of the crystalline phase with respect to the stretching direction, has been formalized
49
50 on a quantitative numerical basis using the usual Hermans orientation function³³
51
52
53

$$\chi = \frac{\overline{3\cos^2\gamma} - 1}{2}$$

54
55
56
57
58
59
60

1
2
3 where $\cos^2\gamma$ is the squared average cosine value of the angle, γ , between the crystallographic c
4 (chain) axes and the stretching direction. The quantity $\cos^2\gamma$ has been experimentally evaluated
5
6 by the intensity of azimuthal distribution of the most intense equatorial reflection (110 for
7 samples with orthorhombic structure and 100 for samples with pseudo-hexagonal structure). In
8 these assumptions, when χ is equal to 1, the c axes of all crystallites are perfectly parallel to the
9 stretching direction while, when χ is equal to 0, there is a random crystallite orientation. For
10 amorphous samples, a degree of axial orientation of polymer chains has been analogously
11 evaluated, by using by the intensity of azimuthal distribution of the amorphous diffraction halo.
12
13
14
15
16
17
18
19
20
21
22

23 Mechanical tests were performed on compression molded samples, kept at 23°C for 24 h. Tensile
24 tests were carried out on a rectangular specimen 50 mm long and 6 mm wide, cut from a 1.5
25 mm-thick compression-molded sheet. The cross head rate was fixed at 500 mm/min.
26
27
28
29
30

31 Tension set measurements were performed according to the ASTM D412 method. The specimen
32 had a 1.5-mm thick, 50 mm-long and 2 mm-wide span. It was held at 200% elongation for 1 min.
33 The tension was then released and measured according to the following formula: $100 ((L_f - L_i)/L_i)$,
34 where L_f and L_i are the final and initial lengths of the specimen, respectively.
35
36
37
38
39
40
41
42
43

44 RESULTS AND DISCUSSION

45
46
47 Effects of the activation conditions on the polymer microstructure.
48
49
50

51 The performance of precatalyst **1** activated by either AlEt_2Cl or MAO under a variety of
52 conditions was evaluated, focusing on the effects of the activation conditions on the polymer
53 microstructure. The polymerization conditions and results of some representative experiments
54
55
56
57
58
59
60

are summarized in Table 1. The data confirm that, under otherwise identical condition, the degree of branching is significantly higher when AlEt₂Cl is used as the activator: e. g. using 1 mmol of Al activator and 1 μmol of Ni, 68 branches per 1000 C's are produced with AlEt₂Cl but only 49 with MAO (cf. entries 2 and 13).²² Interestingly, the degree of branching can be efficiently modulated by proper choice of the AlEt₂Cl amount under identical conditions of temperature and monomer pressure, resulting in the production of PE's containing a variable branching content ranging from 56 branches per 1000 C's at low Al content up to 80 branches per 1000 C's at high Al content (cf. entries 1-5). In comparison, MAO activation under identical conditions results in lower branching densities for all the Al/Ni ratio tested (see entries 11-14). Some influence of the amount of Al activator on the polymer microstructure was previously observed, although apparently contrasting tendencies were reported.²³⁻²⁷ Our findings suggest that a proper choice of the mode of activation is a powerful tool to modulate the polymer microstructure, resulting in larger effects than, e. g., those recently observed when a chemical reductant was added to the same precatalyst.^{34,35}

Table 1. Polymerization conditions and results^{a)}

Entry	Ni cat (μmol)	cocatalyst (mmol)	T (°C)	P (atm)	time (min)	yield (g)	branches ^{b)}
1	1.0	AlEt ₂ Cl (0.5)	20	1	30	1.40	56
2	1.0	AlEt ₂ Cl (1.0)	20	1	30	1.30	68
3	1.0	AlEt ₂ Cl (2.0)	20	1	30	1.51	67
4	3.0	AlEt ₂ Cl (3.0)	20	1	30	2.54	80
5	3.0	AlEt ₂ Cl (2.0)	20	1	60	3.95	76

6	3.0	AlEt ₂ Cl (2.0)	50	1	60	3.75	97
7	1.0	AlEt ₂ Cl (2.0)	20	5	10	3.94	28
8	1.0	AlEt ₂ Cl (2.0)	40	5	7	4.48	49
9	1.0	AlEt ₂ Cl (2.0)	60	5	7	5.10	56
10	1.0	AlEt ₂ Cl (2.0)	80	5	10	2.32	68
11	1.0	MAO (0.5)	20	1	30	0.42	48
12	1.0	MAO (1.0)	20	1	30	0.45	49
13	1.0	MAO (2.0)	20	1	30	1.25	57
14	3.0	MAO (3.0)	20	1	30	2.16	50

^{a)} solvent = toluene 100 mL. ^{b)} Number of branches per 1000 carbons in the polymer chain, including those of the branches, calculated from ¹H NMR.³⁶

We have also investigated the catalyst performance using AlEt₂Cl activation under variable temperature and pressure. As expected from the literature data,^{1,15} the degree of branching increases (and the molecular weight decreases) while the polymerization temperature increases (cf. entries 5 and 6). In particular, a highly branched PE (97 branches per 1000 C's) is obtained at 50 °C, but the sample is sticky due to the low molecular weight (M_w is 87000 compared to 215000 for the sample prepared at 20 °C under the same conditions, see the Experimental section). On the other hand, as expected, an increase of monomer pressure results in a decrease of branching frequency: at 20 °C polymerization temperature, using 2 mmol of AlEt₂Cl and 1 μmol of Ni, the branching content decreases from 67% at 1 atm to 28% at 5 atm (cf. entries 3 and 7). However, proper selection of the values of pressure and temperature allowed us to

1
2
3 produce highly branched, high molecular weight PE samples also under technically more
4 interesting conditions, e.g. at 80 °C (see entry 10).
5
6
7

8
9 Detailed analysis of the polymer microstructures was achieved by ^{13}C NMR analysis according
10 to Galland *et al.*³⁷ The content of branches of different lengths of some representative polymer
11 samples are reported in Table 2. Interestingly, polymers prepared using a higher amount of
12 $\text{Al}(\text{C}_2\text{H}_5)_2\text{Cl}$ as the cocatalyst (such as sample 4, see the ^{13}C NMR spectrum of Figure 1) have a
13 significantly higher content of branches longer than five carbons ("*hexyl+*") and also some
14 "branches on branches" (as indicated by the presence of the "fingerprint" resonances of *sec*-butyl
15 groups). It is also worth noting that in all samples there are significant amounts of neighboring
16 methyls and *hexyl+*'s, i. e. 1,4-dimethyl, 1,5-dimethyl, 1,6-dimethyl and 1,4-dihexyl+, while
17 1,2-dimethyl and 1,3-dimethyl branches, which are always present in ethylene-propylene
18 copolymers, are absent (*v. infra*).
19
20
21
22
23
24
25
26
27
28
29
30
31
32
33
34
35
36
37
38
39
40
41
42
43
44
45
46
47
48
49
50
51
52
53
54
55
56
57
58
59
60

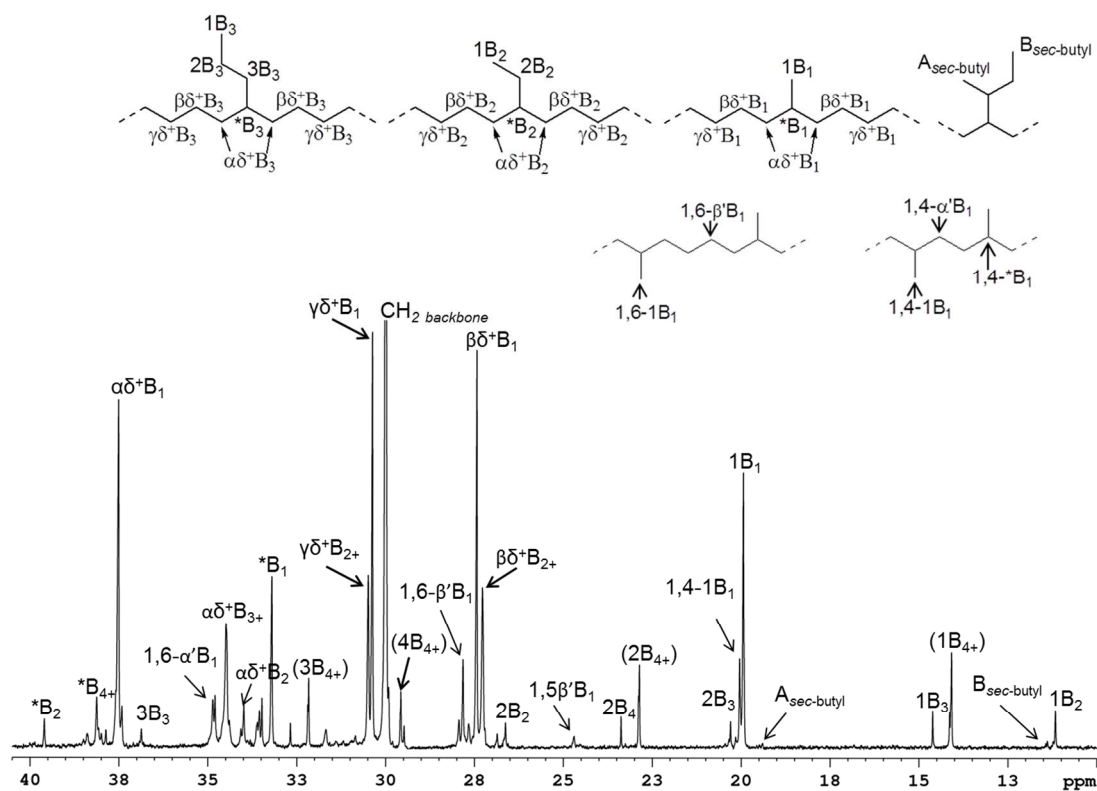


Figure 1. ^{13}C NMR spectrum of a highly branched polyethylene (entry 4).³⁷

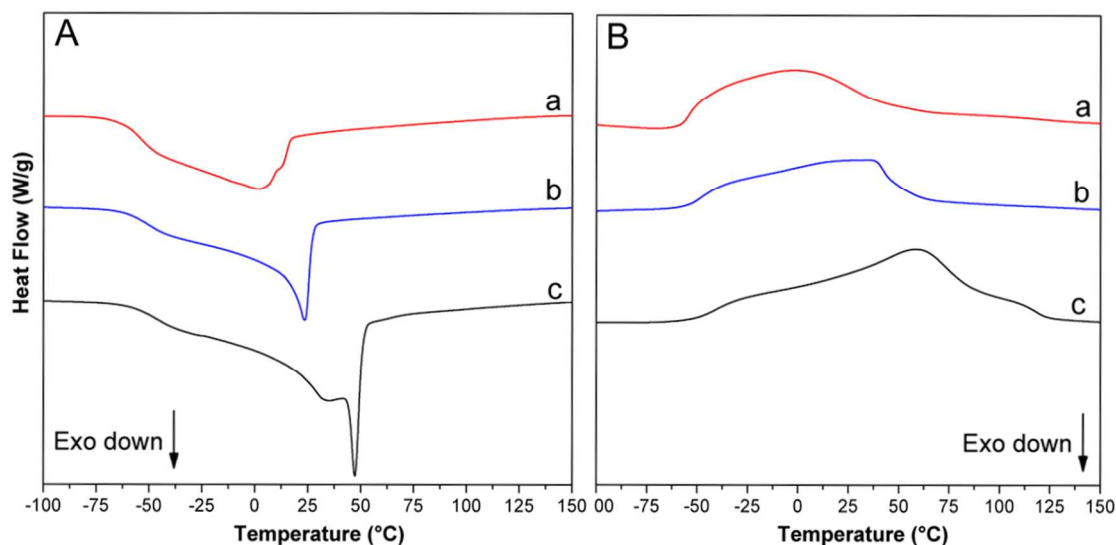
Table 2. Number and type of branches per 1000 carbons evaluated from ^{13}C NMR analysis for some representative samples.

Sample	1,4-Me	1,5-Me	1,6-Me	isolated Me	Et	Pr	Bu	Am	1,4-hexyl+	isolated hexyl+	sec-Bu	total
2	9.3	2.4	10.1	22.6	4.2	2.8	3.1	2.6	2.0	8.7	0.4	68
4	14.1	4.2	15.4	10.4	6.2	2.8	5.6	3.5	6.0	10.2	1.5	80
12	6.0	1.2	4.6	18.5	3.0	1.7	2.3	2.0	1.2	8.4	-	49

Crystallinity of branched polyethylenes

Differential Scanning Calorimetry (DSC) scans of some of the synthesized branched polyethylene samples (hereinafter br-PE) have been collected, after erasing their previous

1
2
3 thermal history by melting at 170 °C in the DSC apparatus. Cooling scans from the melt and
4 subsequent heating scans, both at a rate of 10 °C/min, are shown in Figure 2. As already
5 observed for analogous br-PE samples²⁸ as well as for ethylene copolymers,³⁸⁻⁴² broad
6 endothermic and exothermic peaks are observed that are superimposed to the glass transition
7 temperature. This, of course, reduces the accuracy in evaluation of both temperature and
8 enthalpy of the observed transitions.
9
10
11
12
13
14
15
16
17
18



37 **Figure 2.** DSC scans (A = cooling from the melt; B = second heating) of representative samples
38 of branched PE's, with different number of branching: (a) 80 %; (b) 68 %; (c) 49 %.
39
40
41
42
43
44

45 Melting temperatures (T_m) and enthalpies (ΔH_m), as taken by heating scans like those shown in
46 Figure 2B, are plotted, versus the number of branches per thousand carbon atoms, in Figures 3A
47 and 3B, respectively. For the sake of comparison, T_m and ΔH_m literature values for ethylene
48 random copolymers with propene,⁴¹ 1-octene^{38,41} are also plotted Figure 3. It is apparent that T_m
49 and ΔH_m values observed for br-PE are close to those observed for ethylene copolymers with
50
51
52
53
54
55
56
57
58
59
60

hexyl substituents, while are largely shifted toward lower values of chain branching, with respect to ethylene-propylene random copolymers (exhibiting only methyl substituents along PE chains).

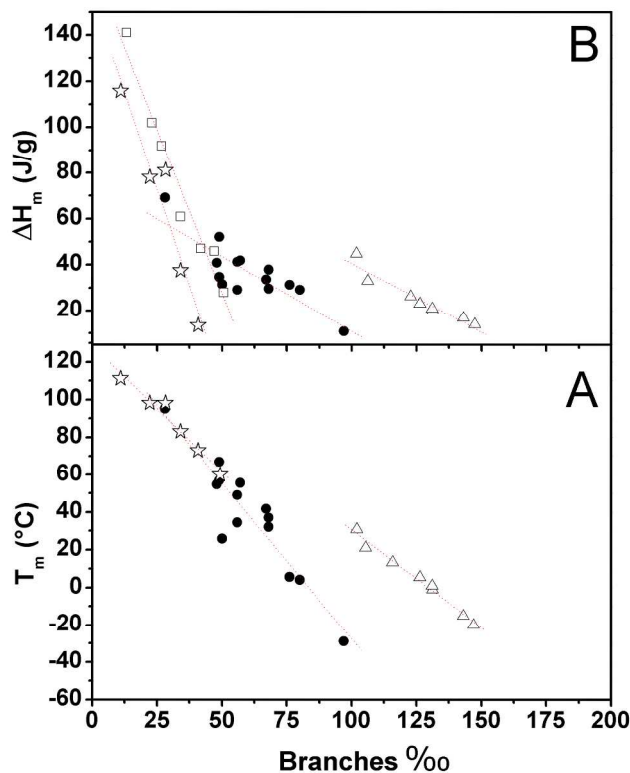
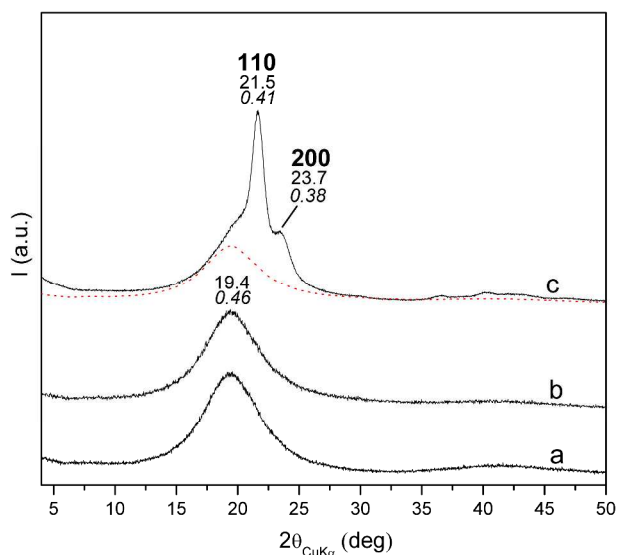


Figure 3. Melting temperatures (A) and melting enthalpies (B) versus the number of branches per thousand carbon atoms, for branched PE samples of Table 1 (dark circles) and, for comparison, of ethene-propene⁴⁰(triangles) and ethylene-octene (squares³⁸ and stars⁴¹) copolymer samples.

Representative WAXD patterns at room temperature, as taken by an automatic powder diffractometer, of br-PE rubbery slabs with different amount of chain branches are collected in Figure 4. For low branching content (e.g., 49 ‰, Figure 4c) crystalline peaks of the

1
2
3 orthorhombic form of polyethylene are clearly present. As the branching content increases, the
4
5 amorphous halo becomes predominant and only an amorphous halo is present for high branch
6
7 content (e.g., 68‰ and 80‰, Figures 4a,b).



32
33 **Figure 4.** WAXD patterns, as taken by an automatic powder diffractometer at room temperature,
34 of branched PE's with different number of branching: (a) 80 ‰; (b) 68‰; (c) 49 ‰.

35
36
37
38
39
40
41
42 Degrees of crystallinity at room temperature derived by WAXD patterns like those of Figure 3,
43 are plotted versus the content of branches and compared with those of random ethylene
44 copolymers with propene⁴⁰ and styrene⁴³ in Figure 5. The complete loss of crystallinity for
45
46 copolymers with propene⁴⁰ and styrene⁴³ in Figure 5. The complete loss of crystallinity for
47
48 branching content higher than 60‰ (Figure 5) is, of course, easily rationalized by the
49
50 corresponding reduction of melting temperature to values lower than room temperature (Figure
51
52
53
54
55
56
57
58
59
60 3).

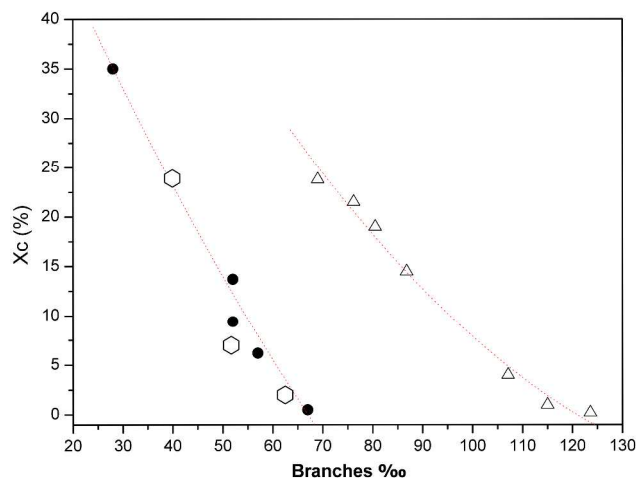


Figure 5. Degree of crystallinity as evaluated by X-ray diffraction patterns at room temperature, versus number of branches per thousand carbon atoms, for branched PE's (dark circles), and, for comparison, for random ethylene-propene⁴¹ (triangles) and ethylene-styrene⁴⁴ copolymers (hexagons).

Of course, for all copolymers, the introduction of substituents in linear polyethylene chains gradually leads to complete loss of crystallinity and hence loss of melting (Figure 2) and diffraction peaks (Figure 4). As expected, minimum disturbance to crystallinity is given by methyl branches, which are able to enter into the lattice of orthorhombic polyethylene, gradually increasing the disorder in the crystalline phase but leaving substantially unaltered the *trans*-planar conformation of the chains.^{44,45} To have a complete loss of crystallinity at room temperature for ethene-propene copolymers, methyl branch content has to be higher than nearly 120‰ (Figure 5, roughly corresponding to ethylene content below 75 mol %). Differently from methyl branches, longer alkyl branches cannot be accommodated in the polyethylene based crystalline phases and as a consequence their presence in polyethylene based chains leads to a more drastic reduction of crystallinity.^{43,46,47} (Figure 4)

1
2
3 X-ray diffraction patterns, like those of Figure 4, also show that unit cell parameters for br-PS
4 samples only slightly increase with branch content. In fact, only increases of **a** and **b** lower than
5
6 1%, with respect to values observed for orthorhombic polyethylene, are observed. An analogous
7
8 behavior has been observed for ethylene copolymers with comonomers bulkier than propene,
9
10 which although produce drastic reduction of crystallinity, cause only minor deformations to the
11
12 orthorhombic unit cell parameters.^{43,46,47}
13
14
15
16
17

18 It is worth adding that although more than one half of branches of br-PE samples are methyl
19
20 groups (Table 2), the observed behavior is completely different from that one observed for
21
22 ethylene-propylene copolymers. In fact, for ethene-propene copolymers, the dimension of the **a**
23
24 axis of the unit cell of polyethylene markedly increases, almost proportionally to methyl
25
26 branches, whereas **b** and **c** axes practically retain the dimensions found in polyethylene. For high
27
28 content of methyl branches, **a** becomes nearly equal to $b \times \sqrt{3}$ and hence the unit cell becomes
29
30 pseudo-hexagonal, where long-range positional order in three dimensions is maintained only for
31
32 chain axes.^{42,44,45} For unstretched br-PE samples formation of an analogous pseudo-hexagonal
33
34 form is not observed.
35
36
37
38
39
40
41
42
43

44 Crystallization under stretching

45
46
47 Variations of X-ray diffraction patterns of br-PE because of room temperature stretching, up to
48
49 strain $\epsilon=4$, are shown in 2D WAXD patterns of Figure 6. Depending on branch content, largely
50
51 different kinds of behavior are observed.
52
53
54
55
56
57
58
59
60

1
2
3 A sample being amorphous at room temperature, with a branching content of 80‰ (and more in
4 general samples with melting temperature roughly in the range -10°C $+10^{\circ}\text{C}$), is reversibly
5 oriented under stretching but remains amorphous (Figure 6A). In fact, the amorphous halo
6 centered at $d=0.46$ nm ($2\theta_{\text{CuK}\alpha} = 19.4^{\circ}$) becomes polarized on the equator, reaching an
7 orientation factor close to $\chi=0.5$ for $\varepsilon=4$, while completely lose its polarization because of stress
8 release (Figure 6A).
9

10
11 A second kind of behavior is that one of an amorphous sample, with a branching of 68‰ (and
12 more in general for samples with melting temperature close to room temperature), that reversibly
13 crystallizes under stretching (Figure 6B). The 2D pattern show the appearance of a well-defined
14 crystalline peak located at $d=0.44$ nm ($2\theta=20.2^{\circ}$), definitely shifted with respect to the
15 maximum of the starting amorphous halo (at $d=0.46$ nm, i.e. $2\theta=19.3^{\circ}$). The patterns of Figure
16 5B also indicate the reversible achievement, for high strain, of a remarkable degree of orientation
17 (for $\varepsilon=4$, $\chi=0.71$).
18

19 A third kind of behavior is that one observed for br-PE sample with 49‰ of branches (and more
20 in general for samples with melting temperature in the range $50-70^{\circ}\text{C}$), which in the unstretched
21 state exhibits an orthorhombic crystalline phase (Figure 6C). As also shown by the pattern of
22 Figure 4, for the unstretched film, an intense 110 diffraction ring at $d=0.41\text{nm}$ and a minor 200
23 diffraction ring at $d=0.37\text{nm}$ are observed. After stretching, already for $\varepsilon=2$, the two
24 orthorhombic crystalline peaks are replaced by a broader diffraction peak centered at $d=0.43\text{nm}$
25 ($2\theta_{\text{CuK}\alpha}=20.6^{\circ}$). The patterns of Figure 6C also indicate the achievement, for high strain ($\varepsilon=4$),
26 of a relatively high degree of orientation ($\chi=0.65$). This kind of crystallinity remains stable even
27 after stress removal, and also its orientation is in part maintained ($\chi=0.37$).
28
29
30
31
32
33
34
35
36
37
38
39
40
41
42
43
44
45
46
47
48
49
50
51
52
53
54
55
56
57
58
59
60

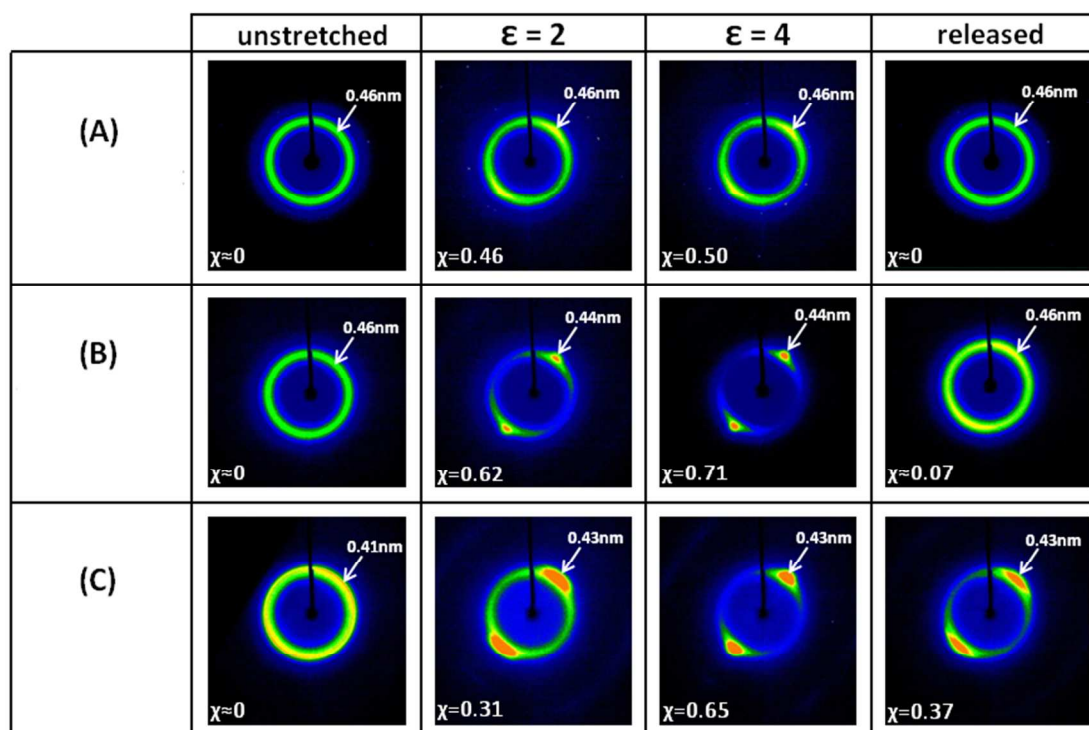


Figure 6. X-ray diffraction patterns ($\text{CuK}\alpha$) as a consequence of room temperature stretching of branched polyethylene samples having: (A) 80% of branching and $T_c = -14^\circ\text{C}$; (B) 68% of branching and $T_c = 33^\circ\text{C}$; (C) 49% of branching and $T_c = 60^\circ\text{C}$.

Finally, br-PE samples with melting temperature higher than 90°C , with a content of branching lower than 30%, have the typical behavior of polyethylene, exhibiting an orthorhombic crystalline form, which irreversibly orients as a function of stretching.

The 2D patterns of stretched samples of Figures 6A and 6B indicate the formation under stretching of a disordered crystalline phase different from the orthorhombic one, both starting from amorphous samples (Figure 6A) as well as from suitable orthorhombic crystalline samples

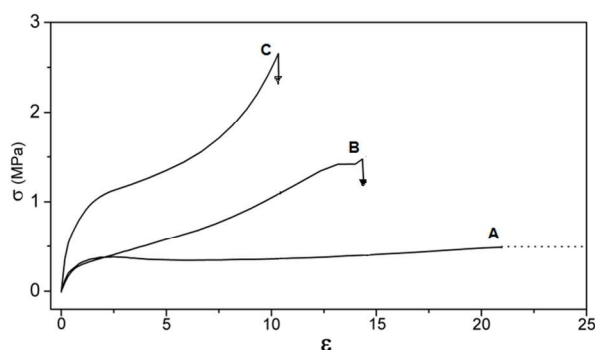
(Figure 6B). The replacement of the two orthorhombic crystalline peaks by a broader diffraction peak centered at higher Bragg distance ($d=0.43-0.44$ nm rather than at 0.41nm) clearly indicates the formation of a pseudo-hexagonal crystallinity⁴³⁻⁴⁸ (with $a = 0.496-0.508$ nm).

Hence, br-PE samples, which roughly include 50% of methyl branches and 50% of bulkier branches, generally exhibit the orthorhombic form as typical of ethylene copolymers with excluded bulk branches. However, as a consequence of stretching, if the branch content is higher than 40%, this orthorhombic form is replaced by a pseudo-hexagonal form, analogous to that one typical of ethylene-propylene copolymers.^{44,45} It is worth adding that this crystallization behavior is particularly similar to that one observed for ethylene-styrene random copolymers, which present only the orthorhombic form in the unstretched state, while a very similar pseudo-hexagonal form has been obtained by stretching of amorphous samples.⁴³

Stress-strain curves and tension set

Typical stress-strain curves at deformation rate of 500mm/min (corresponding to a strain rate of 10 min^{-1}) of the considered br-PE are shown in Figure 7. The observed behavior can be easily rationalized with support of the structural information derived by the X-ray diffraction patterns under stretching of Figure 6. The amorphous samples (e.g. those of Figures 7A and 7B) present rather low and similar elastic moduli ($E = 0.5$ MPa). Amorphous samples that remain amorphous under stretching, only achieving a reversible orientation of the polymer chains in their amorphous phase (Figure 6A) are highly ductile (elongation at break higher than 2000% with stress at break close to 0.4 MPa). Amorphous samples that crystallize under stretching (Figure 6B) exhibit a much higher strength associated with a reduced ductility ($\sigma_B \approx 1.3-1.5$ MPa ; $\epsilon_B \approx$

1
2
3 1500%, Figure 7B). Of course, samples already crystalline in the unstretched state (Figure 6C)
4 exhibit definitely higher elastic moduli ($E = 2$ MPa, Figure 7C). Correspondingly, a further
5 increase of strength and reduction of ductility are observed ($\epsilon_B \approx 1000\%$ and $\sigma_B \approx 2.5$ MPa,
6 Figure 7C).
7
8
9
10
11
12
13



14
15
16
17
18
19
20
21
22
23
24
25
26
27 **Figure 7.** Stress-strain curves at a strain rate of 10 min^{-1} for three branched polyethylene
28 elastomers, with different amount of branching: (A) 80%; (B) 68%; (C) 49%.
29
30
31
32
33
34
35

36 For samples like those of Figure 7, a typical elastomeric behaviour is observed with a low initial
37 modulus and a gradual increase in the slope of stress-strain curves and a large amount of
38 immediate strain recovery after fracture.^{28,49,50} In agreement with a literature study on br-PE,²⁸
39 the transition from localized yielding typical of thermoplastics to uniform stretching typical of
40 elastomers occurred at a degree of crystallinity close to 25%.
41
42
43
44
45
46
47
48

49 A simple quantity suitable to evaluate elasticity of elastomers is the so-called tension set, i.e. the
50 percent of residual increase of sample length ($100 \times (L_f - L_i)/L_i$), after 200% of elongation for 1
51 min. Tension set values, as evaluated for most of the samples of br-PE of Table 1, are shown in
52 Figure 8 versus the amount of chain branching. It is apparent that highest elasticity, i.e. minimum
53
54
55
56
57
58
59
60

values of tension set, are observed for samples that can reversibly crystallize under stretching (like that one of Figure 6B).

Particularly interesting it is also a comparison with tension set data of ethene-propene random copolymers,⁴¹ also plotted in Figure 8. The data of Figure 8 clearly indicate, as T_m and ΔH_m data of Figure 2, that curves for br-PE with respect those of EP copolymers are shifted to much lower values of branching.

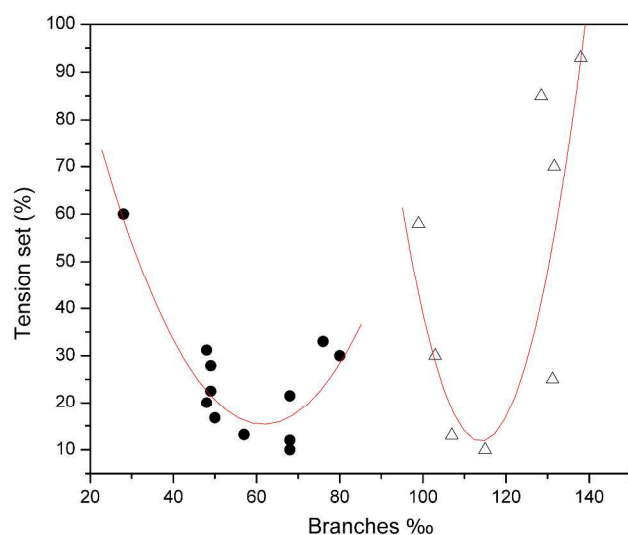


Figure 8. Tension set values versus the amount of branching for branched PE's (dark circles) and, for comparison, for ethylene-propene random copolymers (triangles).

Conclusions

We have re-examined the relationships between the mode of activation of a prototypical Brookhart Ni(II) catalyst and the resulting polyethylene structure. Detailed ^{13}C NMR analysis of the branched polyethylene samples indicated that the polymers prepared under otherwise

1
2
3 identical conditions using AlEt_2Cl instead of MAO as the co-catalyst have a higher content of
4 long chain branches and of "branches on branches". Consequently, high molecular weight
5 amorphous polyethylenes displaying excellent elastomeric properties could be produced under
6 suitable conditions. The relationships between the microstructure and the crystallization behavior
7 and the elasticity of the polymers were studied by DSC, X-ray diffraction and mechanical
8 analyses. For these branched polyethylenes, as for ethylene copolymers, a transition from
9 plastomeric toward elastomeric behaviour occurs as the branch concentration increases. The
10 branch concentration leading to this transition is definitely lower than for ethylene-propylene
11 copolymers while is similar to those observed for ethylene copolymers with bulkier
12 comonomers. For instance, negligible crystallinity at room temperature is reached for branch
13 content of 65% and 115%, for br-PE and EP copolymers, respectively. Analogously, minimum
14 values of tension set, i.e. best elastic response in the absence of covalent crosslinking, are
15 observed for branch content of 65% and 115%, for br-PE and EP copolymers, respectively.
16
17
18
19
20
21
22
23
24
25
26
27
28
29
30
31
32
33
34

35 Hence, for br-PE, elastomeric properties are reached not only using only ethylene but also
36 minimizing branch concentration. For ethylene based elastomeric materials, reduction of branch
37 concentration implies two relevant advantages: i) reduction of glass transition temperature
38 becoming closer to that one of polyethylene; ii) more efficient radical crosslinking with
39 reduction of degradation reactions, typically associated with propene (and other 1-alkene)
40 comonomeric units.
41
42
43
44
45
46
47
48
49
50
51
52
53
54
55
56
57
58
59
60

ACKNOWLEDGEMENTS

Financial support of the “Ministero dell’Istruzione, dell’Università e della Ricerca” is gratefully acknowledged. The authors thank Dr. Ing. Raniero Mendichi of ISMAC, Milan, for SEC analyses.

REFERENCES

- ¹ Johnson, L. K.; Killian, C. M.; Brookhart, M. New Pd(II)- and Ni(II)-Based Catalysts for Polymerization of Ethylene and α -Olefins. *J. Am. Chem. Soc.* **1995**, *117*, 6414-6415.
- ² Guo, L.; Dai, S.; Sui, X.; Chen, C. Palladium and Nickel Catalyzed Chain Walking Olefin Polymerization and Copolymerization . *ACS Catal.* **2016**, *6*, 428-441.
- ³ Hongliang Mu, H.; Li Pan, L.; Song, D.; Li, Y. Neutral Nickel Catalysts for Olefin Homo- and Copolymerization: Relationships between Catalyst Structures and Catalytic Properties. *Chem. Rev.* **2015**, *115*, 12091–12137.
- ⁴ Wang, S.; Redshaw, C.; Sun, W.-H. Recent progress on nickel-based systems for ethylene oligo-/polymerization catalysis. *J. Organomet. Chem.* **2014**, *751*, 717-741.
- ⁵ Baier M. C.; Zuideveld M. A.; Mecking S. Post-Metallocenes in the Industrial Production of Polyolefins. *Angew. Chem. Int. Ed.* **2014**, 9722-9744.
- ⁶ Nakamura, A.; Anselment, T. M. J.; Claverie, J.; Goodall, B.; Jordan, R. F.; Mecking, S.; Rieger, B.; Sen, A.; van Leeuwen, P. W. N. M.; Nozaki, K. Ortho-Phosphinobenzenesulfonate:

1
2
3 A Superb Ligand for Palladium-Catalyzed Coordination–Insertion Copolymerization of Polar
4 Vinyl Monomers. *Acc. Chem. Res.* **2013**, *46*, 1438–1449.

7
8
9 ⁷ Makio, H.; Terao, H.; Iwashita, A.; Fujita, T. FI Catalysts for Olefin Polymerization—A
10 Comprehensive Treatment. *Chem. Rev.* **2011**, *111*, 2363–2449.

13
14
15 ⁸ Delferro, M.; Marks, T. J. Multinuclear Olefin Polymerization Catalysts. *Chem. Rev.* **2011**,
16 *111*, 2450–2485.

19
20
21 ⁹ Lamberti, M.; Mazzeo, M.; Pappalardo, D.; Pellecchia, C. Mechanism of stereospecific
22 polymerization of α -olefins by late-transition metal and octahedral group 4 metal catalysts.
23
24
25 *Coord. Chem. Rev.* **2009**, *53*, 2082–2097.

27
28
29 ¹⁰ Gibson, V. C.; Spitzmesser, S. K. Advances in Non-Metallocene Olefin Polymerization
30 Catalysis. *Chem. Rev.* **2003**, *103*, 283–315.

33
34
35 ¹¹ Coates, G. W. Precise Control of Polyolefin Stereochemistry Using Single-Site Metal
36 Catalysts. *Chem. Rev.* **2000**, *100*, 1223–1252.

38
39
40 ¹² Killian, C. M.; Tempel, D. J.; Johnson, L. K.; Brookhart, M. Living Polymerization of α -
41 Olefins Using NiII– α -Diimine Catalysts. Synthesis of New Block Polymers Based on α -Olefins.
42
43
44
45 *J. Am. Chem. Soc.* **1996**, *118*, 11664–11665.

47
48
49 ¹³ Gates, D. P.; Svejda, S. A.; Oñate, E.; Killian, C. M.; Johnson, L. K.; White, P. S.; Brookhart,
50 M. Synthesis of Branched Polyethylene Using (α -Diimine)nickel(II) Catalysts: Influence of
51 Temperature, Ethylene Pressure, and Ligand Structure on Polymer Properties. *Macromolecules*,
52
53
54
55
56 **2000**, *33*, 2320–2334.

1
2
3 ¹⁴ Guan, Z.; Cotts, P. M.; McCord, E. F.; McLain, S. J. Chain walking: A new strategy to control
4 polymer topology. *Science* **1999**, *283*, 2059.
5
6

7
8
9 ¹⁵ For a comprehensive review, see: Ittel, S. D. and Johnson, L. K. Late-Metal Catalysts for
10 Ethylene Homo- and Copolymerization. *Chem. Rev.* **2000**, *100*, 1169–1203.
11
12

13
14 ¹⁶ For recent leading references, see e. g.: Zhong, L.; Li, G.; Liang, G.; Haiyang Gao, H.; Wu, Q.
15 Enhancing Thermal Stability and Living Fashion in α -Diimine–Nickel-Catalyzed
16 (Co)polymerization of Ethylene and Polar Monomer by Increasing the Steric Bulk of Ligand
17 Backbone. *Macromolecules* **2017**, *50*, 2675–2682.
18
19

20
21 ¹⁷ Zou, W. W.; Chen, C. L. Influence of Backbone Substituents on the Ethylene
22 (Co)polymerization Properties of α -diimine Pd(II) and Ni(II) Catalysts. *Organometallics*, **2016**,
23 *35*, 1794–1801.
24
25

26
27 ¹⁸ Allen, K. E.; Campos, J.; Daugulis, O.; Brookhart, M. Living Polymerization of Ethylene and
28 Copolymerization of Ethylene/Methyl Acrylate Using “Sandwich” Diimine Palladium Catalysts.
29 *ACS Catal.* **2015**, *5*, 456-464.
30
31

32
33 ¹⁹ Du, S.; Kong, S.; Shi, Q.; Mao, J.; Guo, C.; Yi, J.; Liang, T.; Sun, W.-H. Enhancing the
34 Activity and Thermal Stability of Nickel Complex Precatalysts Using 1-[2,6-Bis(bis(4-
35 fluorophenyl)methyl)-4-methyl phenylimino]-2-aryliminoacenaphthylene Derivatives.
36 *Organometallics* **2015**, *34*, 582-590.
37
38

39
40
41 ²⁰ Rhinehart, J. L.; Mitchell, N. E.; Long, B. K. Enhancing α -Diimine Catalysts for High-
42 Temperature Ethylene Polymerization. *ACS Catal.* **2014**, *4*, 2501-2504.
43
44
45
46
47
48
49
50
51

- 1
2
3
4
5
6
7
8
9
10
11
12
13
14
15
16
17
18
19
20
21
22
23
24
25
26
27
28
29
30
31
32
33
34
35
36
37
38
39
40
41
42
43
44
45
46
47
48
49
50
51
52
53
54
55
56
57
58
59
60
- ²¹ Wen, C.; Yuan, S.; Shi, Q.; Yue, E.; Liu, D.; Sun, W.-H. Tailoring Polyethylenes by Nickel Complexes Bearing Modified 1-(2-Benzhydrylnaphthylimino)-2-phenyliminoacenaphthylene Derivatives. *Organometallics* **2014**, *33*, 7223–7231.
- ²² Pappalardo, D.; Mazzeo, M.; Pellicchia, C. Polymerization of ethylene with nickel α -diimine catalysts. *Macromol. Rapid. Commun.* **1997**, *18*, 1017-1023.
- ²³ Kumar, K. R. and Sivaram, S. Ethylene polymerization using iron(II)bis(imino)pyridyl and nickel (diimine) catalysts: effect of cocatalysts and reaction parameters. *Macromol. Chem. Phys.* **2000**, *201*, 1513-1520.
- ²⁴ Simon, L. C.; Williams, C. P.; Soares, J. B. P. and de Souza, R. F. Kinetic investigation of ethylene polymerization catalyzed by nickel-diimine catalysts. *J. Mol. Catal. A Chem.* **2001**, *165*, 55-66.
- ²⁵ de Souza, C. G; de Souza, R. F. and Bernardo-Gusmão, K. Effect of alkylaluminum cocatalyst on ethylene polymerization with nickel- α -diimine complex. *Appl. Catalysis A: General* **2007**, *325*, 87-90.
- ²⁶ Meinhard, D.; Wegner, M.; Kipiani, G.; Hearley, A.; Reuter, P.; Fischer, S.; Marti, O.; Rieger, B. New Nickel(II) Diimine Complexes and the Control of Polyethylene Microstructure by Catalyst Design. *J. Am. Chem. Soc.* **2007**, *129*, 9182-9191.
- ²⁷ Hamedani, N. G.; Arabi, H. A systematic study of Nickel (II) α -diimine complex performance on ethylene polymerization: influence of cocatalyst nature. *Polym. Bull.* **2015**, *72*, 2471-2488.

1
2
3 ²⁸ Thermoelastomeric polymers produced by using Ni(II) catalysts have been reported, see e. g.:
4
5 He, Z. Y.; Liang, Y. R.; Yang, W. H.; Uchino, H. S.; Yu, J. G.; Sun, W.-H.; Han, C. C. Random
6
7 hyperbranched linear polyethylene: One step production of thermoplastic elastomer. *Polymer*
8
9 **2015**, *56*, 119-122.

10
11
12
13 ²⁹ Leone, G.; Mauri, M.; Bertini, F.; Canetti, M.; Piovani, D.; Ricci, G. Ni(II) α -Diimine-
14
15 Catalyzed α -Olefins Polymerization: Thermoplastic Elastomers of Block Copolymers.
16
17 *Macromolecules* **2015**, *48*, 1304–1312.

18
19
20
21 ³⁰ O'Connor, K. S.; Watts, A.; Vaidya, T.; LaPointe, A. M.; Hillmyer, M. A.; Coates, G. W.
22
23 Controlled Chain Walking for the Synthesis of Thermoplastic Polyolefin Elastomers: Synthesis,
24
25 Structure, and Properties. *Macromolecules* **2016**, *49*, 6743–6751.

26
27
28
29 ³¹ tom Dieck, H.; Svoboda, M.; Grieser, T. Z. Bis(diazadien)metall(0)-Komplexe, IV [1]
30
31 Nickel(0)-bis(chelate) mit aromatischen N-Substituenten. *Naturforsch* **1981**, *36b*, 823-832.

32
33
34
35 ³² van Asselt, R.; Elsevier, C. J.; Smeets, W. J. J.; Spek, A. L.; Benedix, R. Synthesis and
36
37 characterization of rigid bidentate nitrogen ligands and some examples of coordination to
38
39 divalent palladium. X-ray crystal structures of bis (*p*-tolylimino) acenaphthene and methylchloro
40
41 [bis(*o,o'*-diisopropylphenyl-imino) acenaphthene] palladium (II). *Recl. Trav. Chim. Pays-Bas*
42
43 **1994**, *113*, 88-98.

44
45
46
47
48 ³³ Alexander, L. E. In: *X-ray Diffraction Methods in Polymer Science*; Krieger, R. E., Ed.;
49
50 Huntington, NY, 1979; Chapter 4, pp 210-211

1
2
3
4
5
6
7
8
9
10
11
12
13
14
15
16
17
18
19
20
21
22
23
24
25
26
27
28
29
30
31
32
33
34
35
36
37
38
39
40
41
42
43
44
45
46
47
48
49
50
51
52
53
54
55
56
57
58
59
60

³⁴ Anderson, W. C.; Rhinehart, J. L.; Tennyson, A. G.; Long, B. K. Redox-Active Ligands: An Advanced Tool To Modulate Polyethylene Microstructure. *J. Am. Chem. Soc.* **2016**, *138*, 774-777.

³⁵ Gao, W.; Xin, L.; Hao, Z.; Li, G.; Su, J-H.; Zhou, L. and Mu, Y. The ligand redox behavior and role in 1,2-bis[(2,6-diisopropylphenyl)imino]-acenaphthene nickel-TMA(MAO) systems for ethylene polymerization. *Chem. Commun.* **2015**, *51*, 7004-7007.

³⁶ As pointed out in: Mader, D.; Heinemann, J.; Walter, P.; Mülhaupt, R. Influence of *n*-Alkyl Branches on Glass-Transition Temperatures of Branched Polyethylenes Prepared by Means of Metallocene- and Palladium-Based Catalysts. *Macromolecules* **2000**, *33*, 1254-1261, different approaches have been used in the literature to calculate the degree of branching, e. g. evaluating from ¹H NMR the number of branching per 1000 carbons in the main chain (methylenes and methines).²⁶ Since the latter approach is not convenient when there is a significant amount of branches longer than methyls, here we calculate the number of branching per 1000 carbons in the polymer chain, including those in the branches, from the intensities of the resonances of methyl, methylene and methine protons in the ¹H NMR spectra.

³⁷ Galland, G. B.; de Souza, R. F.; Mauler, R. S.; Nunes, F. F. ¹³C NMR Determination of the Composition of Linear Low-Density Polyethylene Obtained with [η³-Methallyl-nickel-diimine]PF₆ Complex. *Macromolecules* **1999**, *32*, 1620-1625

³⁸ Bensason, S.; Minick, J.; Moet, A.; Chum, S.; Hiltner, A.; Baer, E. Classification of Homogeneous Ethylene-Octene Copolymers Based on Comonomer Content. *J. Polym. Sci.: Part B: Polym. Phys.* **1996**, *34*, 1301-1315.

- 1
2
3
4
5
6
7 ³⁹ Mathot, V.B.F.; Scherrenberg, R.L.; Pijpers, T.F.J. Metastability and order in linear, branched
8
9 and copolymerized polyethylenes. *Polymer* **1998**, *39*, 4541-4559.
10
11
12 ⁴⁰ Guerra, G.; Ruiz de Ballesteros, O.; Venditto, V.; Galimberti, M.; Sartori, M.; Pucciariello, R.
13
14 Pseudohexagonal crystallinity and thermal and tensile properties of ethene-propene copolymers.
15
16 *J. Polym. Sci., Polym. Phys. Ed.* **1999**, *37*, 1095-1103.
17
18
19
20 ⁴¹ Simanke, A.G.; Galland, G.B.; Freitas, L.; Alziro H. da Jornada, J.; Quijada, R.; Mauler, R.S.
21
22 Influence of the comonomer content on the thermal and dynamic mechanical properties of
23
24 metallocene ethylene/1-octene copolymers. *Polymer* **1999**, *40*, 5489–5495.
25
26
27
28 ⁴² Guerra, G.; Galimberti, M.; Piemontesi, F.; Ruiz de Ballesteros, O. Influence of regio- and
29
30 stereoregularity of propene insertion on crystallization behavior and elasticity of ethene-propene
31
32 copolymers. *J. Am. Chem. Soc.* **2002**, *124*, 1566-1567.
33
34
35
36 ⁴³ Antinucci, S.; Guerra, G.; Oliva, L.; Ruiz de Ballesteros, O.; Venditto V. Pseudo-hexagonal
37
38 crystallinity in ethene-styrene random copolymers. *Macromol. Chem. Phys.* **2001**, *202*, 382-387.
39
40
41
42 ⁴⁴ Bassi, I.W.; Corradini, P.; Fagherazzi, G.; Valvassori, A. Crystallization of high ethylene
43
44 EPDM terpolymers in the stretched state. *Eur. Polym. J.* **1970**, *6*, 709-718.
45
46
47
48 ⁴⁵ Ruiz de Ballesteros, O.; Auriemma, F.; Guerra, G.; Corradini, P. Molecular organization in the
49
50 pseudo-hexagonal crystalline phase of ethylene-propylene copolymers. *Macromolecules* **1996**,
51
52 *29*, 7141-7148.
53
54
55
56
57
58
59
60

1
2
3
4
5
6
7
8
9
10
11
12
13
14
15
16
17
18
19
20
21
22
23
24
25
26
27
28
29
30
31
32
33
34
35
36
37
38
39
40
41
42
43
44
45
46
47
48
49
50
51
52
53
54
55
56
57
58
59
60

⁴⁶ Vonk, C. G.; Reynaers, H. Interpretation of variations in the unit cell dimensions of polyethylene. *Polymer Commun.* **1990**, *31*, 190-193.

⁴⁷ Rizzo, P.; Baione, F.; Guerra, G.; Martinotto, L.; Albizzati, E. Polyethylene unit cell and crystallinity variations as a consequence of different cross-linking processes. *Macromolecules* **2001**, *34*, 5175-5179

⁴⁸ Vanden Eynde, S.; Rastogi, S.; Mathot, V. B. F.; Reynaers, H. Ethylene-1-Octene Copolymers at Elevated Pressure-Temperature. 1.Order-Disorder Transition. *Macromolecules* **2000**, *33*, 9696-9704

⁴⁹ Baldwin, F. P.; Ver Strate, G. Polyolefin Elastomers Based on Ethylene and Propylene. *Rubber Chem. Technol.* **1972**, *45*, 709-881

⁵⁰ Bensason, S.; Stepanov, E.V. ; Chum, S.; Hiltner, A.; Baer, E. Deformation of Elastomeric Ethylene-Octene Copolymers. *Macromolecules* **1997**, *30*, 2436-2444

Table of Contents Graphic

Title:

Efficient modulation of polyethylene microstructure by proper activation of (α -diimine)Ni(II) catalysts: synthesis of well performing polyethylene elastomers.

Authors:

Ilaria D'Auria, Mario Maggio, Gaetano Guerra,* and Claudio Pellecchia*

